remote sensing

MDPI

Article

Time-Lagged Correlation between Soil Moisture and Intra-Annual Dynamics of Vegetation on the Mongolian Plateau

Li Na [1,2], Risu Na [3], Yongbin Bao [1] and Jiquan Zhang [1,2,*]

[1] School of Environment, Northeast Normal University, Changchun 130024, China; lin152@nenu.edu.cn (L.N.); baoyb924@nenu.edu.cn (Y.B.)
[2] Key Laboratory for Vegetation Ecology, Ministry of Education, Changchun 130024, China
[3] School of Geographical Sciences, Northeast Normal University, Changchun 130024, China; nars582@nenu.edu.cn
* Correspondence: zhangjq022@nenu.edu.cn; Tel.: +86-135-9608-6467

Abstract: Soil moisture is a reliable water resource for plant growth in arid and semi-arid regions. Characterizing the interaction between soil moisture and vegetation is important for assessing the sustainability of terrestrial ecosystems. This study explores the spatiotemporal characteristics of four soil moisture layers (layer 1: 0–7 cm, layer 2: 7–28 cm, layer 3: 28–100 cm, and layer 4: 100–289 cm) and the time-lagged correlation with the normalized difference vegetation index (NDVI) for different vegetation types on an intra-annual scale on the Mongolian Plateau (MP). The most significant results indicated that: (1) the four layers of soil moisture can be roughly divided into rapid change (layers 1 and 2), active (layer 3), and stable (layer 4) layers. The soil moisture content in the different vegetation regions was forest > grassland > desert vegetation. (2) The soil moisture in layer 1 showed the strongest positive correlation with NDVI in the whole area; meanwhile, the soil moisture of layers 2 and 3 showed the strongest negative correlation with the NDVI mainly in grassland and desert, and layer 4 showed the strongest negative correlation with the NDVI in the forest. (3) Mutual responses of NDVI and deep layer soil moisture required a longer time compared with the shallow layer. In the annual time scale, the NDVI was affected by the change in soil moisture in most of the study area, except for coniferous forest and desert vegetation regions. (4) Under the different stages of vegetation change, the soil moisture changes advance than NDVI about 3 months during the greening stage, while the NDVI changes advance than soil moisture by 0.5 months during the browning stage. Regardless of the stage, changes in soil moisture are initiated from the shallow layer and advance to the deep layer. The results of this study provide deep insight into the relationship between soil moisture and vegetation in arid and semi-arid regions.

Keywords: soil moisture; different vegetation types; arid and semiarid regions; phenology period

Citation: Na, L.; Na, R.; Bao, Y.; Zhang, J. Time-Lagged Correlation between Soil Moisture and Intra-Annual Dynamics of Vegetation on the Mongolian Plateau. *Remote Sens.* **2021**, *13*, 1527. https://doi.org/10.3390/rs13081527

Academic Editor: Iñigo Molina

Received: 26 February 2021
Accepted: 12 April 2021
Published: 15 April 2021

1. Introduction

Soil moisture is an important driver of the productivity and sustainability of terrestrial ecosystems [1,2], and a limiting factor for plant transpiration and photosynthesis, which determines the vegetation type and structure during ecological construction, particularly in arid and semiarid regions [3]. At the same time, vegetation in an ecosystem controls the soil moisture distribution pattern [4], and affects soil moisture to varying degrees in two opposing aspects through the ecological functions of water storage and conservation, and the absorption and consumption of soil moisture [5,6]. Plant biological processes also affect soil moisture content [7,8]. Different plant species cause different rainfall-runoff and evaporation, thereby inducing spatial distribution of soil moisture at various depths and different hydraulic properties [9,10]. Generally, we hope to discover the time-lagged correlation between soil moisture and vegetation, e.g. the correlation at the various soil depths, under the different vegetation types, and in different growth stages of vegetation,

etc. These quantified data are of great importance for a deeper understanding of the regional soil moisture-vegetation relationship.

Relationships between soil moisture and vegetation in a semi-arid region can be divided into three categories, i.e., correlation, synergism and trade-off [11]. Currently, there are two opposing theories concerning the effects of vegetation on soil moisture [12]. Meanwhile, water fixation of vegetation maintains a high level of soil moisture, however, vegetation growth requires water consumption, which reduces soil moisture [13,14]. Soil moisture exhibits spatial heterogeneity in horizontal and vertical directions due to the influence of vegetation community structure and distance from the canopy [15]. Forest and shrub canopies mediate soil moisture fluctuations by reducing evaporative losses, through shade, and rainfall inputs, through canopy interception, thereby buffering extreme fluctuations in soil moisture in the upper soil profile [16,17]. The water conservation function in alpine grasslands has been previously determined, and there is a significant correlation between vegetation coverage and soil moisture [18]. Zhang et al. found that the above-ground biomass and litter quality of natural grassland communities in the semi-arid region of the Loess Plateau were significantly positively correlated with soil moisture content, and species diversity and richness are increased with soil moisture content [19].

Vegetation affects evapotranspiration through water consumption and energy balance. Previous research has indicated that different vegetation types have spatiotemporal heterogeneity of water uptake patterns at different depths, which can directly affect the dynamic changes in the growing season [20–22]. The correlation between soil moisture content in the 0–20 cm soil layer with evapotranspiration of meadow grassland with 95% average coverage was higher than that of desert grassland with less than 15% vegetation coverage [23]. Pueyo et al. investigated the effects of plant spatial distribution and composition on water infiltration capacity and runoff in semiarid grasslands in Spain, and reported a negative correlation between soil capillary water adsorption capacity and vegetation aggregates in bare land patches. Plant roots determine soil water redistribution and carbon absorption in plant systems [24]. Previous studies have shown that soil moisture decline in a part of the Losses Plateau after the Grain-for-Green Program (GFGP) were initiated at the end of the 1990s to reconvert croplands to forests, shrubs, and grass [2,25,26]. The effect of the root system on soil water repellency is greater than that of waxy leaves, which can reduce the soil infiltration rate and soil water storage, promote surface runoff, and ultimately reduce system productivity [27]. Conversely, too high soil moisture levels will reduce transpiration; for example, high organic soils may become saturated in tropical mountain forests [28], or frequent floods in mangrove swamps [29]. In summary, there are limited studies on the intra-annual time-lagged correlation between vegetation and soil moisture at different depths, and hence the interaction between them warrants further investigation.

The Mongolian Plateau (MP) is the largest arid/semi-arid plateau in the Northern Hemisphere and is located in the inland plateau of central Asia. Its natural ecological environment is fragile and sensitive to global climate change [30]. Soil moisture plays a key role in ecological development as an important water storage resource in the MP. Therefore, it is important to investigate the relationship between soil moisture and vegetation for the entire Eurasian terrestrial ecosystem. However, there is a lack of data on the relationship between soil moisture and vegetation in the Mongolian Plateau. Guo (2010) reports that remote-sensing data were used to retrieve soil moisture to establish a quantitative monitoring system for soil moisture in the MP [31], while Wei et al. discussed the response of soil moisture to climatic factors and vegetation in the MP [32]. The relationship between soil moisture and dust emissions shows that soil moisture can control dust events in the Bayan-Unjuul of Mongolia [33].

In this study, we analyze the spatiotemporal distribution characteristics of soil moisture at various depths and the time-lagged correlation with the normalized difference vegetation index (NDVI) at different stages of vegetation changes under different vegetation types. The primary objectives of this study are to: (1) investigate the spatiotemporal distribution characteristics of soil moisture at various depths; (2) analyze the time-lagged

correlation between the soil moisture at various depths and NDVI of different vegetation types; (3) discuss the relationship between the soil moisture at various depths and NDVI at different stages of vegetation changes across the MP. The results of this study contribute to the sustainable management of terrestrial ecosystems in the MP and other similar regions.

2. Materials and Methods

2.1. Study Area

The study area ranged over the Mongolian Plateau (MP) (87°43′–126°04′E and 37°22′–53°20′N), covering the entire Mongolian People's Republic and the Inner Mongolia Autonomous Region of China, with an area of 2.74 × 10^6 km^2 [30] and an elevation of 85–4203 m (Figure 1). This region is the largest arid/semi-arid plateau in the Northern Hemisphere, and obvious zonality is produced by the distribution of hydrothermal conditions, which is prompted by the differences in the geographical location and underlying surface [34]. The regional mean annual precipitation is approximately 300–400 mm, which decreases from north to south and east to west. The MP's mean temperature is between −1.7 and 5.6 °C, and is characterized by a large temperature difference between day and night, abundant sunlight, strong ultraviolet radiation, gales, and fast weather changes [35,36].

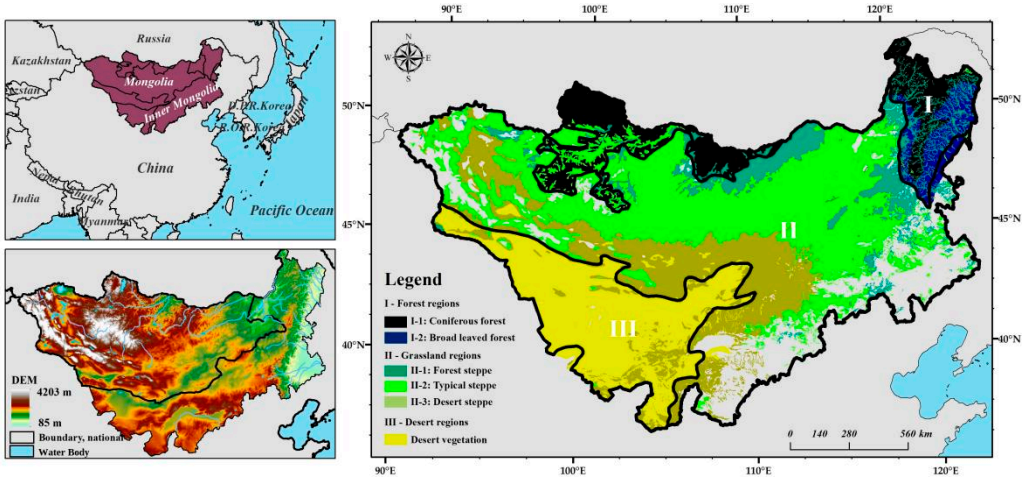

Figure 1. Locations of the Mongolian Plateau (MP), elevation, and vegetation types.

The ecosystem is mainly composed of grassland (70%) [37], with relatively small areas of forests in the north and northeast, shrubs in the south and southeast, farmland and sparse vegetation in the Gobi desert, and sandy areas in the southwest, which form an important and unique geographical landscape of Eurasia [30]. Therefore, we divided the vegetation into three primary types namely, I: forest, II: grassland, and III: desert vegetation, and further classified them into secondary types namely I-1, coniferous forest; I-2, broad-leaved forest; II-1, forest steppe; II-2, typical steppe; II-3, desert steppe [38]. The MP serves as an important and ideal region for research on the response of arid and semi-arid ecosystems to global climate change [39].

2.2. Data Sources

The monthly average soil moisture data were acquired from the fifth and latest global climate reanalysis datasets (ERA5). The dataset was produced by the European Centre for Medium-Range Weather Forecasts (ECMWF, after the First Global Atmospheric Research Program [GARP] Global Experiment [FGGE], the ECMWF Reanalysis 15 [ERA15], the ECMWF Reanalysis 40 [ERA40], and ERA-Interim). ERA5 has been available since 1979, at a spatial resolution of 0.25° × 0.25°, and provides several atmospheric, land-surface, and sea-state parameters on an hourly basis. Compared with ERA-Interim, the ERA5 4D-Var data assimilation system in the Integrated Forecasting System (IFS Cycle 41r2) has been

improved with several modifications, representing a decade of research and development in modeling and data assimilation. The ERA soil moisture dataset was validated against the available data from multiple sources, and the use of this dataset for testing model simulations on daily to seasonal time scales has been confirmed [40,41]. In this study, we used the ERA5 soil moisture data from 1982 to 2015, and the depths of the four soil layers ranged from 0 to 7, 7–28, 28–100, and 100–289 cm, respectively. To calculate the correlation between soil moisture and vegetation, we used the resample tool of the raster processing module in ArcGIS10.5, which is consistent with the spatial resolutions of soil moisture and NDVI. In order to improve the spatial resolution of the data, the soil moisture data were resampled to 8 km using the bilinear resampling mode selected in this study. The bilinear calculates the value of each pixel by averaging (weighted for distance) the values of the surrounding four pixels, which is suitable for continuous data.

Precipitation and evaporation data were obtained from the ERA5 dataset.

The Global Inventor Modeling and Mapping Studies (GIMMS) NDVI3g data (1982–2015) were used to explore the time-lagged correlation with soil moisture. The NDVI dataset was obtained from the GIMMS group of the US National Oceanic and Atmospheric Administration's Advanced Very High-Resolution Radiometer (AVHRR). The dataset had a spatial resolution of 8 × 8 km and a temporal resolution of 15 days [42]. It has been shown to be more accurate for monitoring vegetation activity and phenological changes [43].

2.3. Methods

2.3.1. Data Smoothing and Up-Sampling

The multi-year averages for the 15-day NDVI and monthly soil moisture data were calculated. The resolution of the time series data of the NDVI and soil moisture at intra-annual stages must be unified, for which the monthly soil moisture data were up-sampled to a 15-day temporal resolution. First, the Whittaker smoother was used [44], followed by Fourier interpolation to increase the sampling of the soil moisture data [45]. Then, the original monthly-scale time-series data were transformed to the frequency domain, and the sampling points (filling the blank values) were expanded in the frequency domain series. Finally, inverse Fourier transformation was used to increase the sampling to a 15-day time scale (1–24 periods).

2.3.2. Time-Lagged Correlation Analysis

In this study, based on the 15-day soil moisture and NDVI data, the maximum correlation coefficient, and the lag time between the two were calculated using time-lagged correlation analysis [45]:

(1) First, the correlation coefficients between NDVI and soil moisture were calculated for different time lags as follows:

$$r_k(x,y) = \frac{\sum_{i=1}^{n-k}(x_i - \overline{x}_i)(y_{i+k} - \overline{y}_{i+k})}{\sqrt{\sum_{i=1}^{n-k}(x_i - \overline{x}_i) \cdot \sum_{i=1}^{n-k}(y_{i+k} - \overline{y}_{i+k})}} \quad (1)$$

where $r_k(x,y)$ refers to the series of correlation coefficients between the NDVI and soil moisture under time lag k, x_i and y_i are the series of soil moisture and NDVI, respectively; n is the length of the series; and k is the time lag (k = 0, ±1, ±2, ...), where $k \leq n/4$. As the correlation analysis used 15-day interval data at an annual scale (n = 24), the maximum value of k was 6 (6 × 15 = 90 days).

(2) Next, the maximum values of the correlation coefficients for each time lag were calculated as follows:

$$r_1(k_1) = \max(r_1(x, y)) \tag{2}$$

$$r_2(k_2) = \min(r_k(x, y)) \tag{3}$$

$$\begin{array}{c} R = r_1, K = k_1 | r_1 | > | r_2 | \\ R = null, K = null | r_1 | = | r_2 | \\ R = r_2, K = k_2 | r_1 | < | r_2 | \end{array} \tag{4}$$

where r_1 is the maximum value of the correlation coefficient between the NDVI and soil moisture under time lag k_1; r_2 is the minimum value of the correlation coefficient between the NDVI and soil moisture under time lag k_2, and R and K refer to the extremum value and time lag of the cross-correlation between the NDVI and soil moisture, respectively.

Within this, $k > 0$ indicates that the soil moisture change affects the NDVI variation; $k < 0$ indicates that the NDVI change affects soil moisture variations; and $k = 0$ indicates synchronous intra-annual changes in soil moisture and NDVI.

2.3.3. Defining the Different Stages of Vegetation Change

To identify the relationship between the soil moisture and NDVI at different stages of vegetation change, the phenological nodes of the vegetation were further extracted. Firstly, a curve was fitted for the cumulative NDVI based on a regression logistic model, which was first proposed by Zhang et al. [46].

$$y(t) = \frac{c}{1 + e^{a+bt}} + d \tag{5}$$

where $y(t)$ is the cumulative NDVI at day t, d is the initial background NDVI value, and c is the difference between the maximum and minimum cumulative NDVI values. Therefore, $c + d$ is the maximum cumulative NDVI, while a and b are the fitting parameters [47]. According to the fitting curve, the greening stage of the vegetation was from January to August (Figure 2a) while the browning stage was from August to December (Figure 2b).

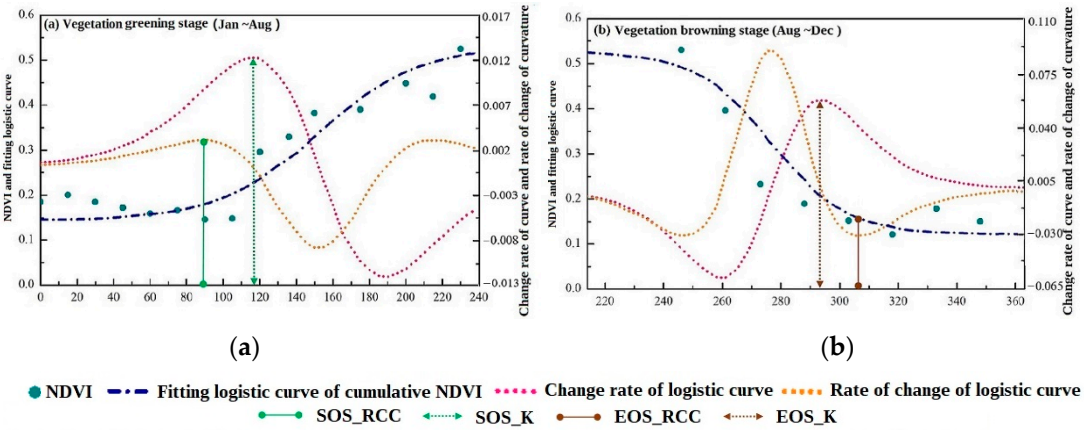

Figure 2. Illustration of the cumulative normalized difference vegetation index (NDVI) on the MP based on logistic regression curves. The change curves of cumulative NDVI in vegetation greening stage (**a**) and vegetation browning stage (**b**). (The SOS_RCC is start of the growing season; EOS_RCC is end of the growing season; SOS_K is maximum curvatures of the stage of vegetation greening and the EOS_K is minimum curvatures of the stage of vegetation browning).

Next, according to the curvature curve [46,47] and curvature extremum [48] of the cumulative NDVI logistic fitted curve method, the maximum (SOS_K) and minimum

curvatures (EOS_K) of the vegetation greening and browning stages on the MP were calculated (Figure 2) as follows:

$$k = \frac{da}{ds} = -\frac{b^2cz(1-z)(1+z)^3}{\left[(1+z)^4 + (bcz)^2\right]^{1.5}} \quad (6)$$

where $z = e^{a+bt}\alpha$ is the angle (in radians) of the unit tangent vector at time t along a differentiable curve, and s is the unit length of the simulated NDVI curve.

Finally, the rate of curvature change (RCC) method [49] was used to define the corresponding times for the maximum curvature change rate during the greening stage as the start of the growing season (SOS_RCC) and the minimum curvature change rate during the browning stage at the end of the growing season (EOS_RCC).

$$RCC = b^3cz\left\{\frac{3z(1-z)(1+z)^3\left[2(1+z)^3 + b^2c^2z\right]}{\left[(1+z)^4 + (bcz)^2\right]^{2.5}} - \frac{(1+z)^2(1+2z-5z^2)}{\left[(1+z)^4 + (bcz)^2\right]^{1.5}}\right\} \quad (7)$$

where a, b, c, and z represent the same values as in Equations (5) and (6).

3. Results

3.1. Spatiotemporal Distribution of the Soil Moisture in Mongolian Plateau (MP)

3.1.1. Spatial Distribution of the Soil Moisture at Various Depth

Figure 3 shows the spatial distribution of mean annual soil moisture at various depths during 1982–2015 across the MP. The spatial distribution of average multi-annual soil moisture content ranged from 0 to 0.469 m^3/m^3 and with an average of 0.18 m^3/m^3 at layer 1; in layer 2, the soil moisture content of 0 to 0.459 m^3/m^3 and with an average of 0.18 m^3/m^3; in layer 3, the soil moisture content of 0 to 0.459 m^3/m^3 and with an average of 0.20 m^3/m^3; in layer 4, the soil moisture content of 0 to 0.448 m^3/m^3 and with an average of 0.21 m^3/m^3. In the vertical distribution, the area of soil moisture content <0.1 m^3/m^3 in layer 1 and layer 2 is relatively large, accounting for 30% and 29%, respectively. The area of soil moisture content range of 0.2–0.3 m^3/m^3 in layer 3 is relatively large, accounting for 41%. However, area of soil moisture range of 0.1–0.2 m^3/m^3 and 0.3–0.4 m^3/m^3 in the layer 4 is relatively large, accounting for 37% and 18%, respectively. In general, the soil moisture content increased with increasing depth. The soil moisture contents in layers 1 and 2 were relatively lower than those in layers 3 and 4. In the horizontal distribution, the soil moisture decreased from east to west and from north to south in each layer. The spatial heterogeneity was obvious, which was consistent with the distribution of different vegetation types in the MP. Among them, the soil moisture content was highest in vegetation type I, which was higher than 0.3 m^3/m^3, followed by the soil moisture content in the II vegetation type area, which was approximately 0.2–0.3 m^3/m^3 in II-1 vegetation type, 0.1–0.3 m^3/m^3 in II-2 vegetation type, and less than 0.2 m^3/m^3 in II-3 vegetation type. The soil moisture content in the III vegetation type was the lowest, with a content of less than 0.1 m^3/m^3. The order of the soil moisture contents at different depths for the different vegetation types was I > II (II-1 > II-2 > II-3) > III.

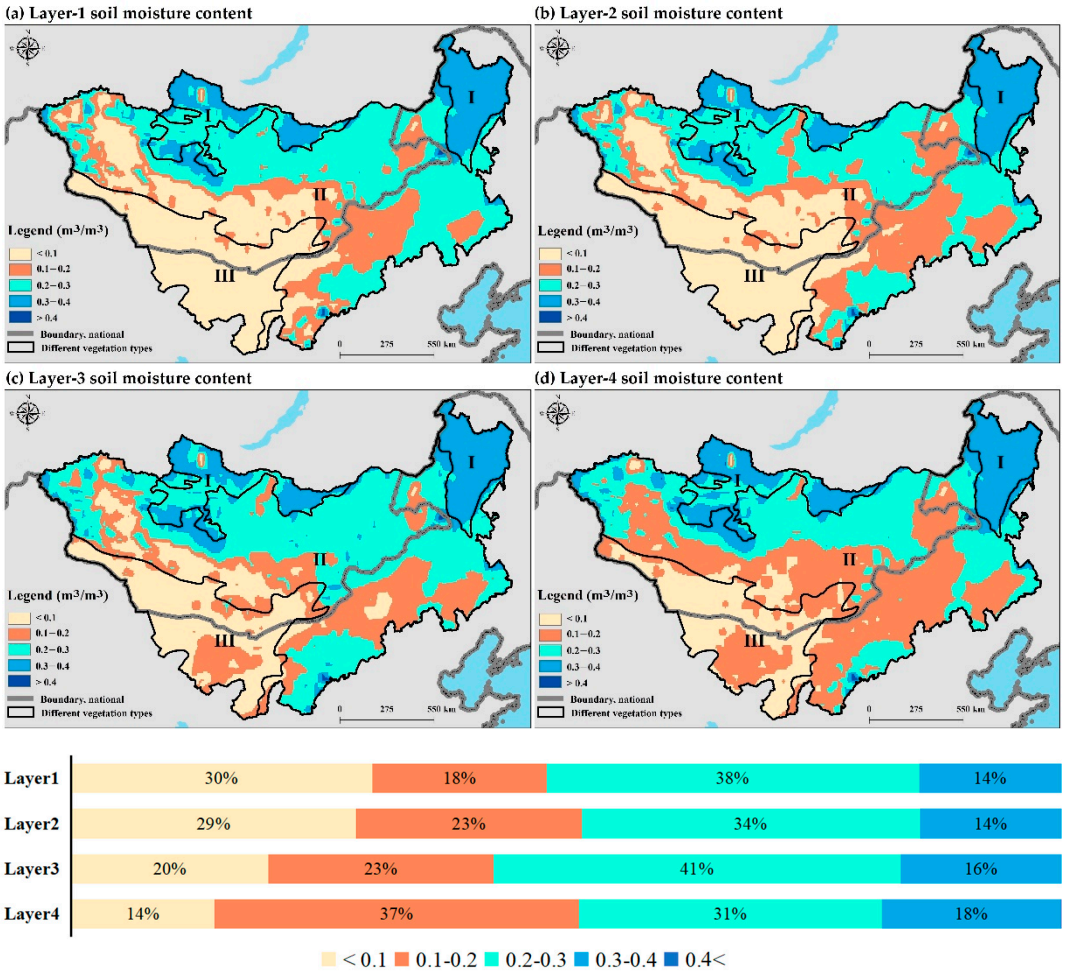

Figure 3. Spatial distribution of mean annual soil moisture at various depths during 1982–2015 across the MP. The (**a**–**d**) represent the layer 1, layer 2, layer 3 and layer 4, respectively.

3.1.2. Temporal Distribution of the Soil Moisture at Various Depth

Data smoothing and up-sampling methods were used to process the soil moisture data on a daily scale. Figure 4 shows the variations in soil moisture over an average period between 1982 and 2015 at various depths in intra-annual at daily scale across the MP. The uniformity and stability of the soil moisture increased with depth, which is the soil moisture volatility at layers 1, 2, and 3, and the stability in layer 4 was obvious. Among them, the change trends of the soil moisture in layers 1 and 2 are similar, showing an "up-down-up-down" trend. Changes in soil moisture in layer 1 showed an upward trend from the beginning of 0.164 m^3/m^3 increase to the first peak value (0.184 m^3/m^3) on day 75, and then decreased to the valley value (0.165 m^3/m^3) on day 125. Then, it peaked (0.205 m^3/m^3) on day 210 intra-annual and subsequently showed a downward trend. The changes in soil moisture in layer 2 were slightly delayed compared to those in layer 1. Corresponding to the increasing period of soil moisture in layer 1, the soil moisture in layer 2 decreased from 0.172 m^3/m^3 to 0.166 m^3/m^3. Subsequently, it increased to 0.172 m^3/m^3 on day 95. Then, it decreased to the lowest value of 0.158 m^3/m^3 on day 130, and increased to the highest value of 0.205 m^3/m^3 on day 225, followed by a downward trend. Changes in soil moisture in layer 3 were opposite or delayed to those in layers 1 and 2. The variation trends of soil moisture in layer 3 showed the "down-up-down-up-down" trend. From the original 0.206 m^3/m^3, it increased to 0.203 m^3/m^3, and decreased rapidly to the lowest value of 0.191 m^3/m^3 on day 165. Subsequently, soil moisture increased to 0.202 m^3/m^3 on day 230, and showed a short-term downward trend, while the second valley value was 0.197 m^3/m^3 around day 275 and showed an upward trend until day 327, with the highest

value of 0.207 m^3/m^3 in intra-annual. The change in soil moisture in layer 4 was relatively stable, ranging from 0.204 to 0.206 m^3/m^3, with the highest value of 0.206 m^3/m^3 on days 175 to 275.

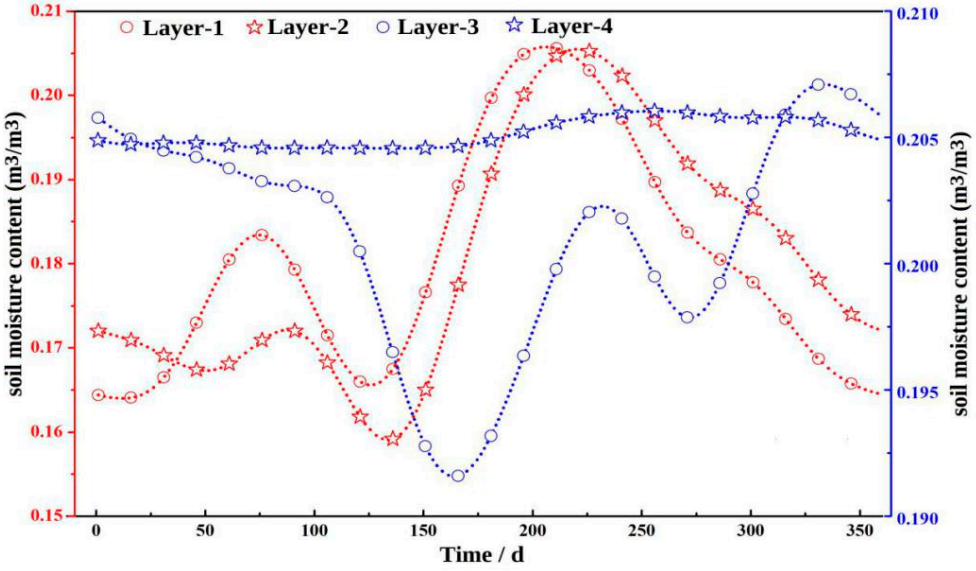

Figure 4. Trends of daily soil moisture an average of the 1982–2015 year at various depths in MP.

3.2. Spatial Characteristics of the Time-Lagged Correlation between NDVI and Soil Moisture

The extremum correlation coefficient and lag time between NDVI and soil moisture at various depths in different vegetation types are shown in Figure 5. Regarding the time-lagged correlation between the soil moisture and NDVI in layer 1 (Figure 5(a-1,a-2)), the extremum correlation coefficient was positively correlated with the lag time according to the spatial distribution. When the extremum correlation coefficient was positive, the lag time was positive; otherwise, it was negative. For layer 1, the positive correlation between NDVI and soil moisture accounted for 86% of the area. The NDVI was affected by soil moisture and accounted for 64% ($1< k < 3$), mainly distributed in the II-1 and II-2 vegetation regions. The synchronization between the changes in the soil moisture and NDVI accounted for 22% ($k = 0$), mainly distributed in vegetation areas II-3 and III. The negative correlation between the NDVI and soil moisture was 14% ($-3 < k < -1$), mainly distributed in vegetation region I. For layer 2, the positive correlation between the NDVI and soil moisture was 45%, and the negative correlation was 55% (Figure 5(b-1,b-2)). The NDVI was affected by soil moisture, accounting for 45% ($1< k < 2$) and was mainly distributed in the I and II-1 vegetation regions. In comparison, the NDVI change the soil moisture area, occupying 55% of the study area, and the lag time was comparatively longer ($-6 < k < -4$), and was mainly distributed in the II-2, II-3, and III vegetation types. For layer 3, the negative correlation between the NDVI and soil moisture accounted for 78%, while 22% of the area showed a positive correlation (Figure 5(c-1,c-2)). The area of soil moisture affecting the NDVI change accounted for 69%. Among them, the NDVI lag change than soil moisture was 1-3 months for the II-2 and II-3 vegetation types and 0.5 month in the I type. The area in which the NDVI change affected the soil moisture accounted for 26%, with a comparatively longer lag time ($-4 < k < -2$), mainly distributed in vegetation types II-1 and III. In addition, the area in which the changes in the soil moisture and NDVI were synchronized accounted for 5% ($k = 0$). For layer 4, the areas of positive and negative correlations between the NDVI and soil moisture accounted for 59% and 41%, respectively (Figure 5(d-1,d-2)). Among them, the area of NDVI affected by the soil moisture was mainly distributed in I-2 and II vegetation types, and the lag times in I-2 and II vegetation types were $k = 6$ and $1 < k < 4$, respectively. The area of soil moisture affected by NDVI was mainly distributed in vegetation types I-1 and III, and the lag time $k = -6$. The time-lagged correlation between

the NDVI and soil moisture at various depths was different on an intra-annual scale in the different ecological regions of the MP. Therefore, in this study, different vegetation cover types were used to analyze the interrelationship between NDVI and soil moisture at various depths.

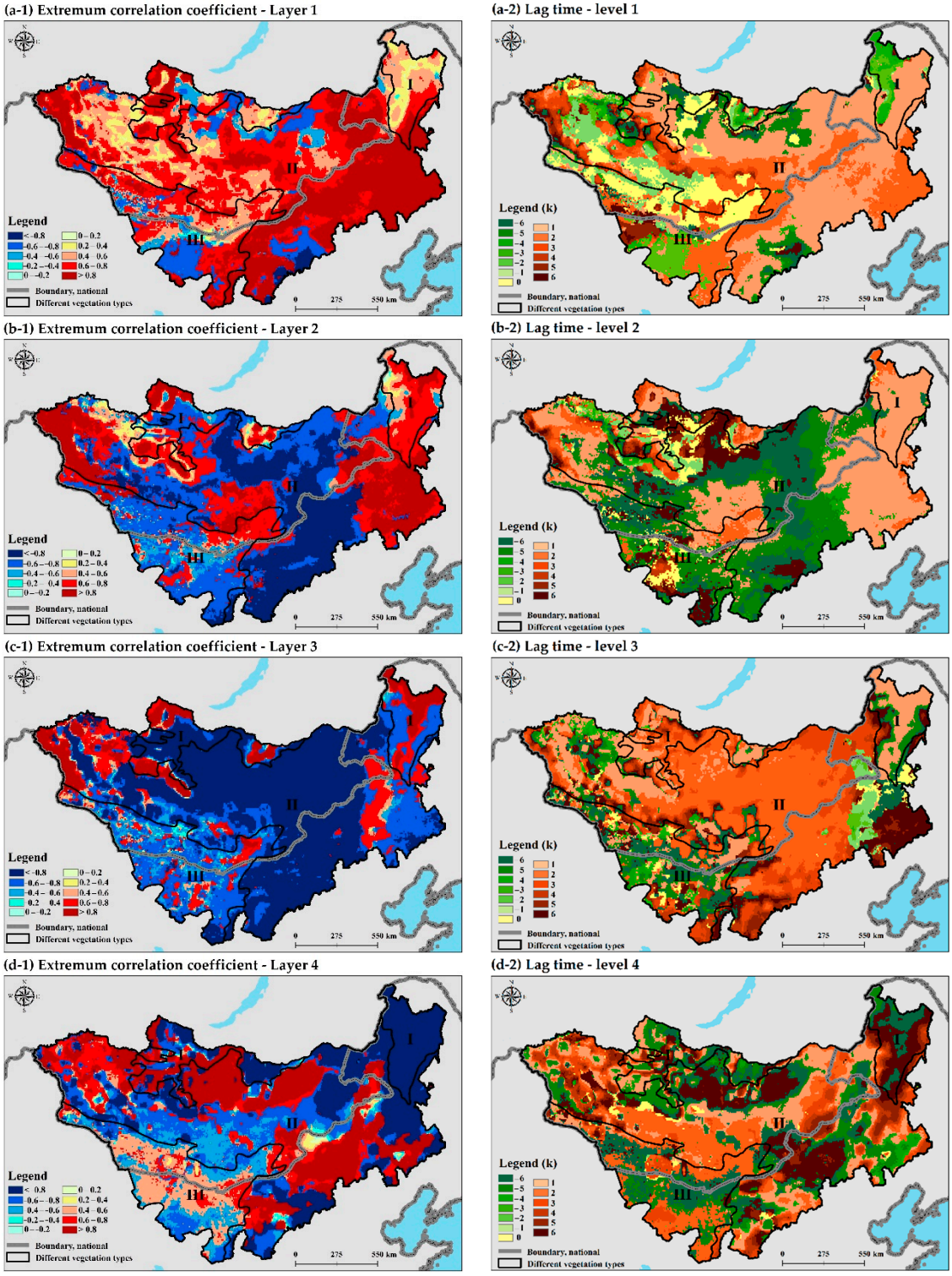

Figure 5. Spatial distribution of the extremum correlation coefficients (**a-1**,**b-1**,**c-1**,**d-1**) and lag time (**a-2**,**b-2**,**c-2**,**d-2**) between the NDVI and soil moisture at various depths across the MP.

Furthermore, we used the different vegetation types on the MP to calculate the mean value of the extremum correlation coefficient and time lag between the soil moisture at various depths and NDVI (Figure 6a). The NDVI and layer 1 soil moisture were positively correlated in all vegetation types; the extremum correlation coefficient in II-2 and II-3 vegetation types was the highest, followed by the I, II-2, and III regions, respectively. There was a positive correlation between layer 2 soil moisture and NDVI in regions I and II-1, and the extremum correlation coefficient was high, with a negative correlation in the II-2, II-3, and III regions, but the extremum correlation coefficient was low. There was a negative correlation between layer 3 soil moisture and NDVI, and the extremum correlation coefficient in region II was the highest, followed by regions III, I-2, and I-1. The correlation between layer 4 soil moisture and NDVI was negative in regions I and II-1, and in I-2 had the highest correlation, while the II-2, II-3, and III regions had a positive correlation, and the extremum correlation coefficient was low.

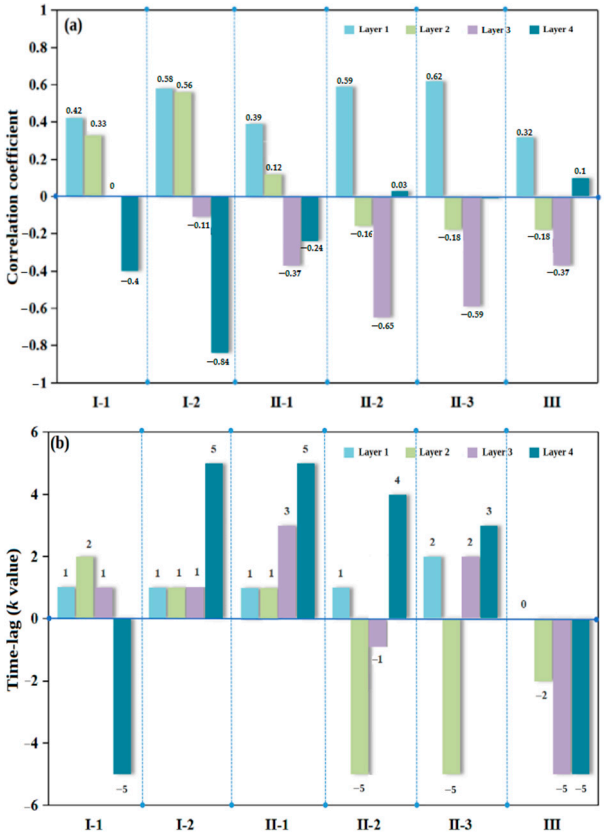

Figure 6. Extremum correlation coefficient (**a**) and lag time (**b**) between the NDVI and soil moisture at various depths for different vegetation types.

The time lag between NDVI and soil moisture at various depths is shown in Figure 6b. Soil moisture changes in layers 1 and 2 affect the NDVI (k = 1–2) in regions I and II, and layer 1 soil moisture synchronous changes with NDVI in III. Layer 2 soil moisture was affected by the NDVI changes in regions II-2, II-3, and III, while soil moisture change lag was longer than NDVI in II-2 and II-3 (k = −5) and shorter in III (k = −2). Layer 3 soil moisture change affected the NDVI in regions I, II-1, and II-3, and NDVI changes lag time was shorter (k = 1–3). The NDVI change affected the soil moisture in regions II-2 and III; among them, the soil moisture change lag time was shorter in II-2 (k = −1) and longer in III (k = −5). Layer 4 soil moisture change affected the NDVI in I-2 and II regions, and NDVI changes lag time was longer (k = 3–5). The NDVI change affected the soil moisture in the I-1 and III regions, while the soil moisture change lag time was longer (k = −5).

3.3. Temporal Characteristics of the Time-Lagged Correlation between NDVI and Soil Moisture

3.3.1. Variations Trend of NDVI and Soil Moisture at Different Stages of Vegetation Change

The maximum change curvature of NDVI and soil moisture at different stages of vegetation change was obtained using the logistic fitted curve method. The NDVI continued to increase during the vegetation greening stage (Figure 7a). Corresponding to the start of the growing season (SOS_RCC) on around day 90, the layer 1 soil moisture curve showed the highest decrease curvature (layer 1_-k), while the layer 2 soil moisture curve showed the highest decrease curvature (layer 2_-k) on day 110. As the NDVI changed to the highest increased curvature (SOS_k/NDVI_k) on day 115, layer 1 soil moisture presented the lowest valley in the year, while the layer 3 soil moisture change curve presented the highest decrease curvature (layer 3_-k). With the continuous increase in NDVI, the soil moisture declined rapidly in layer 3, and showed an upward trend in layers 1 and 2. The soil moisture in layers 1 and 2 showed the highest upward curvature on day 152 (layer 1_k) and day 162 (layer 2_k), respectively. The corresponding soil moisture in layer 3 decreased to its lowest value on day 165, and then showed an upward trend. On day 200, with the soil moisture rapidly increasing in layer 3 (layer 3_k), the soil moisture of layer 4 also showed an obvious upward trend. At the same time, the soil moisture in layer 1 had the highest value of the year. The curvature of the soil moisture change curve in layer 4 was smaller during the entire vegetation greening stage.

The NDVI continued to decrease during the vegetation browning stage (Figure 7b). With the rapid decline of NDVI, the soil moisture change curve of layer 3 showed the highest decrease in curvature (layer 3_-k) on day 250. On day 260, the highest decreasing curvature of the soil moisture change curve of layer 1 (layer 1_-k) was observed, which corresponded to the highest decreasing curvature of the NDVI curve (NDVI_-k). The highest decreased curvature of the soil moisture change curve of layer 2 was observed on day 270 (layer 2_-k). Subsequently, the soil moisture in layer 3 increased rapidly after day 275. The change curve of soil moisture in layer 3 showed the highest increasing curvature (layer 3_k), and the soil moisture in layer 4 showed a downward trend corresponding to the end of the growing season (EOS_RCC).

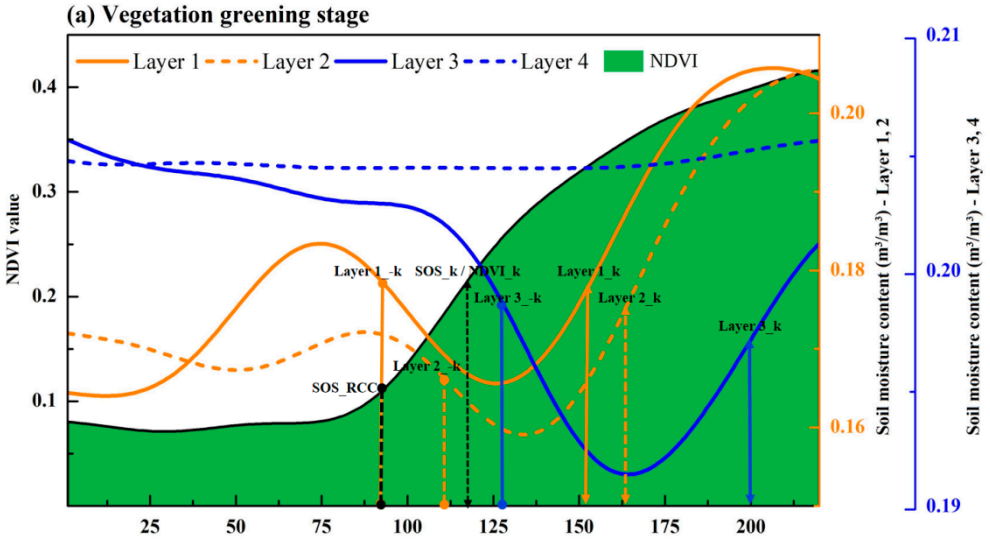

Figure 7. *Cont.*

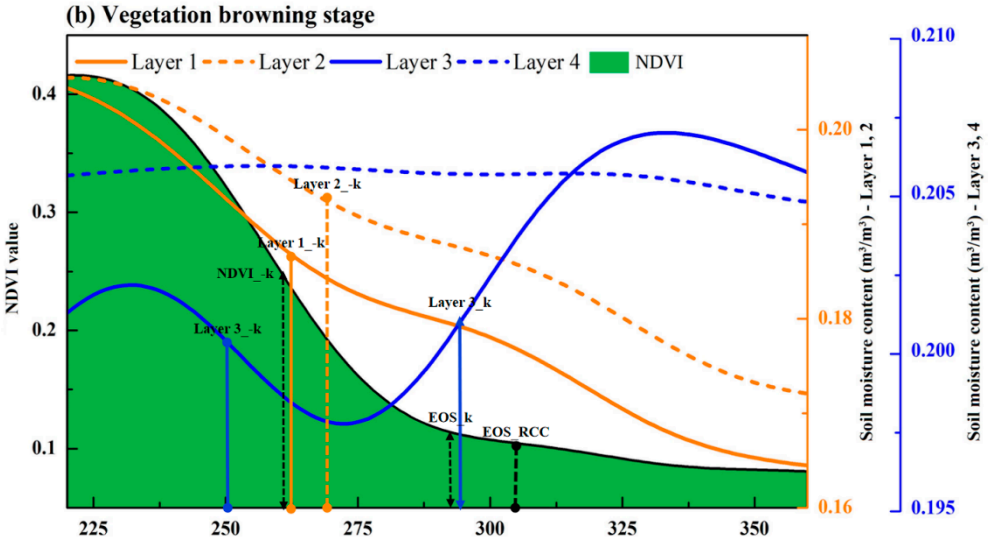

Figure 7. Change curve of the NDVI and soil moisture in vegetation greening stage (**a**) and vegetation browning stage (**b**) in intra-annual across the MP.

3.3.2. Time-Lagged Correlation between the NDVI and Soil Moisture at Different Stage of Vegetation Changes

In this study, we investigated the time lag between the changes in the NDVI and soil moisture at various depths in different stages of vegetation changes using the statistics of the pixel number proportion (Figure 8). In the greening stage, the soil moisture in layer 1, 2, 3 changes advance than NDVI about 3 months ($k = -6$). However, there were differences in the relationship between the NDVI and soil moisture at various depths in the different vegetation types during the browning stage. The change of layer 1 soil moisture lagged than NDVI by 0.5–1 months ($k = 1, 2$) in I and II regions, and 3 months ($k = 6$) in III region. The change of layer 2 soil moisture lagged NDVI by 0.5 month ($k = 1$), except for regions II-2 and III. The changes in the NDVI and soil moisture were synchronized ($k = 0$) in region II-2, while the NDVI changes were lagged 2 months ($k = -4$) with those of the soil moisture in region III. The changes in the NDVI and soil moisture at layer 3 differed between the individual vegetation types. The changes in the NDVI lagged behind the soil moisture by 1 month ($k = -2$) in region I-1, and changes advance about 0.5 month ($k = 1$) and 2.5 months ($k = 5$) in I-2, III regions and II region, respectively. The NDVI changes advanced soil moisture at layer 4 in the greening stage, while the NDVI lagged behind the soil moisture changes in the browning stage. However, the changes in the NDVI and soil moisture in layer 4 were obviously synchronized in region III.

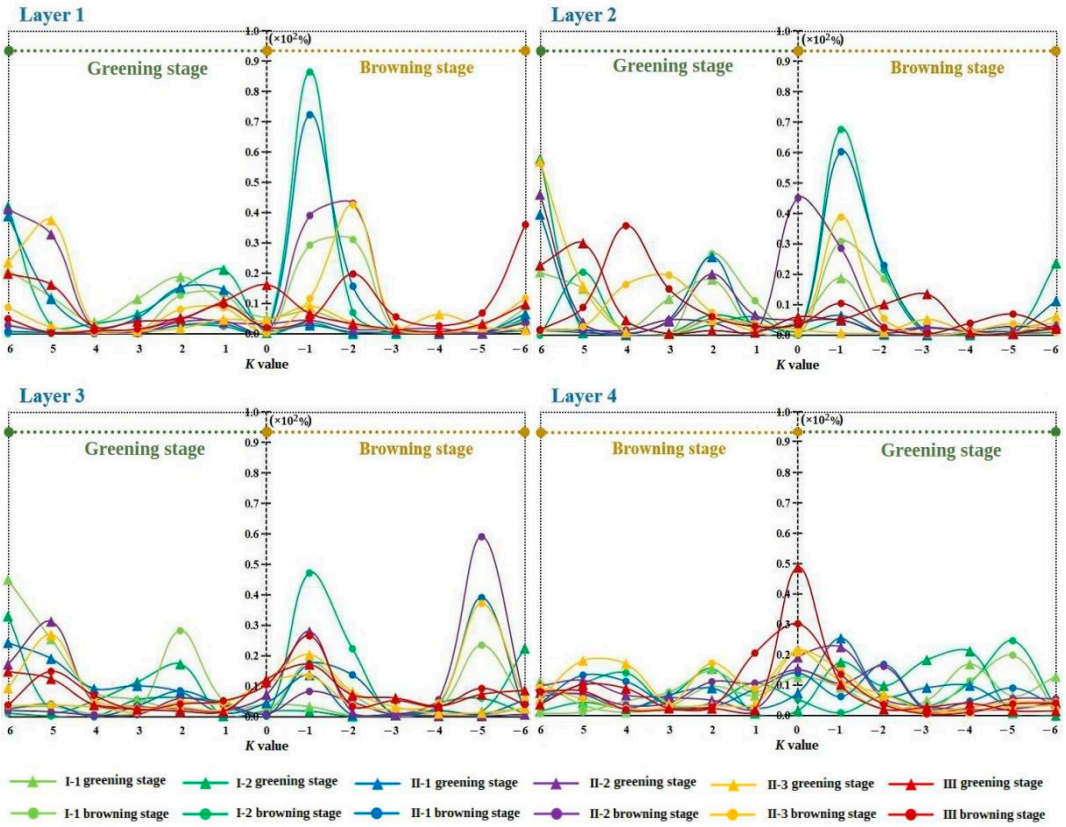

Figure 8. Pixel number proportion of the time lag between the NDVI and soil moisture at various depths during the different stages of vegetation change (Note: the positions of the greening and browning stages are in accordance with the pixel number proportions).

4. Discussion

4.1. Spatiotemporal Characteristics of the Soil Moisture in MP

On the vertical scale, according to the four-layer soil moisture distribution of intra-annual, the soil moisture can be roughly divided into the rapid change (layers 1 and 2), active (layer 3), and stable (layer 4) layers [50]. Across the MP, the uniformity and stability of the soil moisture increased with depth. Similar results were found by Zhao et al. in the Loess Plateau, China [51]. To further illustrate the relationship between the soil moisture at various depths and precipitation/evaporation according to the different vegetation types, a partial correlation analysis was performed (Figure 9) due to the susceptibility of soil moisture to rainfall, vegetation transpiration, and soil evaporation [52,53]. It was found that the precipitation and evaporation correlation with soil moisture decreased with increasing depth. Among them, there was a positive correlation with the soil moisture in layer 1 and layer 2, and the correlation coefficient was higher in layer 1 than layer 2. The negative correlation with soil moisture in layer 3 and layer 4, and the correlation coefficient was higher in layer 3 than layer 4. The above results agree with previous studies that the immediate effects of external factors on soil moisture are weakened by soil depth, thus ensuring that the soil moisture in deeper layers is less disrupted [54–56].

On the horizontal scale, the correlation coefficient between the precipitation/ evaporation and soil moisture in layers 1 and 2 was higher than in layers 3 and 4 in region I. The deep rooting pattern of trees, unlike other plants, allows for the movement of water from deep to shallow soil horizons [9]. This specific water pumping property, known as hydraulic lifting [57,58], can have an important ecological role in terms of water redistribution in soils [59]. We found significant differences in the relationship between precipitation and soil moisture in the different forest types. The I-1 region is mainly distributed in high latitudes, where the temperature is relatively low, little evaporation and less precipitation.

At the same soil type, the root system of I-2 is deeper and more developed, and can infiltrate the water into the deep soil layer following precipitation, therefore, the soil moisture of this area is easily disturbed by precipitation and highly correlated with precipitation compared with the I-1 region [60].

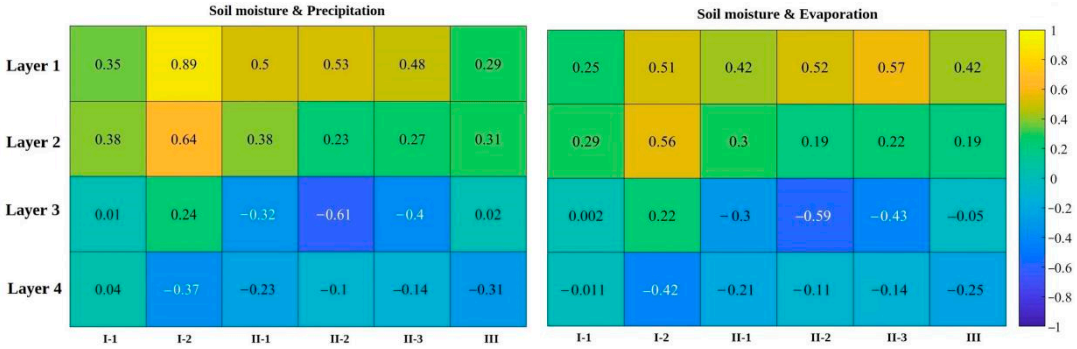

Figure 9. Partial correlation coefficient between the precipitation (**a**), evaporation (**b**), and soil moisture at various depths for different vegetation types.

In the II-2 region, the negative correlation coefficient between precipitation/ evaporation and layer 3 soil moisture is higher than that of other layers, primarily due to the same period of the hydrothermal and growing season in the study area [49]. The results indicated that the soil moisture in layer 3 was the most important water source during plant growth in the II-2 region. However, the correlation between soil moisture and evaporation was higher than that with precipitation in regions II-3 and III. Evaporation is highly sensitive to variations in soil moisture in arid and semi-arid regions [61].

On the temporal scale, the soil moisture content was higher from June to October, which shows the regularity of soil water consumption in late spring and early summer, soil water accumulation in late summer and early autumn, and soil water consumption in late autumn and early winter, which is consistent with previous findings [62,63].

4.2. Relationship between the Soil Moisture and NDVI in MP

The analysis of the time-lagged correlation between the NDVI and soil moisture at various depths showed significant differences in the interaction characteristics of different ecological communities. The strongest positive correlation between the NDVI and soil moisture was in layer 1, which was mainly attributed to the simultaneous effects of precipitation and water fixation by vegetation. Conversely, the strongest negative correlation between the NDVI and soil moisture in the forest was in layer 4, while that for grassland and desert vegetation was in layer 3. This was attributed to the widely penetrating roots of desert and grassland vegetation within the 0–70 cm soil layer [64], and the forest roots deeper than 100 cm [65] on the MP (Figure 10). We also found that the correlation between two different forest types was different in the same soil layer, mainly due to the different root distribution depths of the two forest types. Since previous studies have shown that coinciding with rooting patterns, the soil water content at 50 and 70 cm depth remains low in the I-1, where coarse roots are found in deeper soil horizons, more water is directed deeper in the II-2 [60]. Mutual responses of NDVI and soil moisture in the deep layer required a longer time compared with the shallow layer. This is mainly due to the small change in deep layer soil moisture, which makes the vegetation insensitive to changes. In the annual time scale, the NDVI is affected by the change of soil moisture in most areas of the study area, except for I-1 and III regions. This results due to the less precipitation and low groundwater level in I-1 and III regions, thereby these regions are rarely disturbed by external factors. Studies have shown that the soil moisture "memory" increases with depth

that in the top 1 m layer being 2.5 months in northern China [66], so the deeper layer's soil moisture is not sensitive to changes in NDVI.

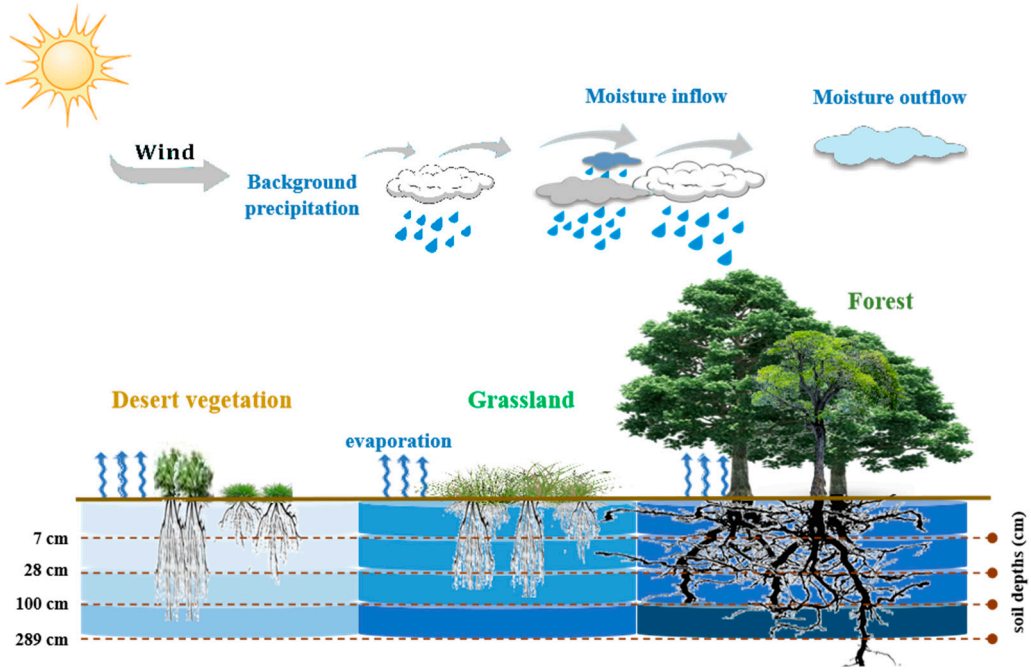

Figure 10. Schematic diagram of relationship between the NDVI and various depth soil moisture under different vegetation types.

However, the correlation between the NDVI and soil moisture at various depths in different vegetation types is associated with the root length and water consumption intensity during the different stages of vegetation changes [45]. For example, at the start of the growing season (SOS_RCC), on day 90, the soil moisture in layers 1 and 2 began to decline, indicating that vegetation growth requires water absorption, which mainly comes from the shallow soil layers. When the vegetation growth reached the highest rate (SOS_K), on day 115, the soil moisture in layers 1 and 2 reached the minimum value during the year, while that in layer 3 began to decline rapidly. This shows that vegetation requires significant water consumption during the rapid growth stage, and when the soil moisture supply of layers 1 and 2 becomes insufficient, water is absorbed from the soil moisture of layer 3 [67]. To a certain extent, the soil moisture also began to increase with vegetation growth, which indicates that the increase in vegetation changed the surface albedo and Bowen ratio, precipitation and water fixation by the dense vegetation [13,14]. At the start of the browning stage, the soil moisture in layers 1 and 2 began to decline a few days earlier than the NDVI. When the browning rate reached its highest point, the soil moisture simultaneously increased in layer 3 and decreased in layer 4. Due to the weakened water fixation effect and larger evaporation during autumn, which leads to the rapid loss of soil moisture in the shallow layers, the soil moisture in layer 4 moves to the upper layers for evaporation [68]. We also found that the changes in soil moisture at each level during the browning stage were less dynamic and decreased at a constant rate in comparison with that during the greening stage. This is mainly because the speed of soil thawing in spring is greater than the speed of freezing in autumn [69].

5. Conclusions

In this study, we investigated the spatiotemporal characteristics of soil moisture at various depths and the time-lagged correlation between with NDVI according to the different stages of vegetation changes in different vegetation types on the MP. We found that the uniformity and stability of soil moisture increased with depth, indicating the fine

soil moisture conditions of the deepest layer. According to the four layers, soil moisture change characteristics can be roughly divided into the rapid change layers (layer 1 and 2), active layer (layer 3) and stable layer (layer 4). The soil moisture content increased with the value of NDVI, which indicated that the vegetation is one of the important controlling factors of the soil moisture spatial distribution.

The extremum correlation between the soil moisture at various depths and NDVI showed that the strongest positive correlation between with NDVI and soil moisture at layer 1 in all vegetation types and has the highest correlation coefficient in desert steppe region. Except for the coniferous forest region, the negative correlation between with NDVI and soil moisture at layer 3 in the study area, especially the highest correlation in typical steppe region. The soil moisture at layer 4 has a higher negative correlation between NDVI in forests than other vegetation types, and in particular the highest in boreal-leaved forest. These results indicate that the length of plant roots determines the different correlations between with NDVI and different layers soil moisture.

Mutual responses NDVI and soil moisture in the deep layer required a longer time than the shallow layer. In the annual time scale, the NDVI is affected by the change of soil moisture in most areas of the study area, except for coniferous forest and desert vegetation regions. In different stages of vegetation change, the soil moisture changes advance NDVI about 3 months in the greening stage, while the NDVI changes advance soil moisture by 0.5 months in the browning stage. Regardless of which stage of vegetation changes, the changes of soil moisture start from the shallow layer, then to deep layer. In addition, the peak and valley values of soil moisture changes intra-annually are very consistent with the vegetation phenology period and, therefore, the annual changes in the soil moisture can be used as an important basis for the extraction of the phenological features of vegetation.

Author Contributions: L.N., conceptualization, methodology, writing—original draft; J.Z., conceptualization, supervision; R.N., writing—review and editing; Y.B., software. All authors have read and agreed to the published version of the manuscript.

Funding: This research was funded by the International (Regional) Cooperation and Exchange Programs, grant number 41961144019.

Institutional Review Board Statement: Not applicable.

Informed Consent Statement: Not applicable.

Data Availability Statement: Not applicable.

Conflicts of Interest: The authors declare no conflict of interest.

References

1. Legates, D.R. Soil moisture: A central and unifying theme in physical geography. *Prog. Phys. Geogr.* **2011**, *35*, 65–86. [CrossRef]
2. Yang, L.; Wei, W.; Chen, L.; Chen, W.; Wang, J. Response of temporal variation of soil moisture to vegetation restoration in semi-arid Loess Plateau, China. *Catena* **2014**, *115*, 123–133. [CrossRef]
3. Engstrom, R.; Hope, A.; Kwon, H.; Stow, D. The Relationship Between Soil Moisture and NDVI Near Barrow, Alaska. *Phys. Geogr.* **2008**, *29*, 38–53. [CrossRef]
4. Hupet, F.; Vanclooster, M. Intraseasonal dynamics of soil moisture variability within a small agricultural maize cropped field. *J. Hydrol.* **2002**, *261*, 86–101. [CrossRef]
5. Wu, W.; Geller, M.A.; Dickinson, R.E. The Response of Soil Moisture to Long-Term Variability of Precipitation. *J. Hydrometeorol.* **2002**, *3*, 604–613. [CrossRef]
6. Wang, A.; Shi, X. A Multilayer Soil Moisture Dataset Based on the Gravimetric Method in China and Its Characteristics. *J. Hydrometeorol.* **2019**, *20*, 1721–1736. [CrossRef]
7. Coenders-Gerrits, A.M.J.; Van Der Ent, R.J.; Bogaard, T.A.; Wang-Erlandsson, L.; Hrachowitz, M.; Savenije, H.H.G. Uncertainties in transpiration estimates. *Nat. Cell Biol.* **2014**, *506*, E1–E2. [CrossRef] [PubMed]
8. Chang, L.L.; Dwivedi, R.; Knowles, J.F.; Fang, Y.H.; Niu, G.Y.; Pelletier, J.D.; Rasmussen, C.; Durcik, M.; Barron-Gafford, G.A.; Meixner, T. Why Do Large-Scale Land Surface Models Produce a Low Ratio of Transpiration to Evapotranspiration? *J. Geophys. Res. Atmos.* **2018**, *123*, 9109–9130. [CrossRef]
9. Aranda, I.; Forner, A.; Cuesta, B.; Valladares, F. Species-specific water use by forest tree species: From the tree to the stand. *Agric. Water Manag.* **2012**, *114*, 67–77. [CrossRef]

10. Cubera, E.; Moreno, G. Effect of land-use on soil water dynamic in dehesas of Central-Western Spain. *Catena* **2007**, *71*, 298–308. [CrossRef]
11. Wang, L.; Wang, X.; Chen, L.; Song, N.-P.; Yang, X.-G. Trade-off between soil moisture and species diversity in semi-arid steppes in the Loess Plateau of China. *Sci. Total Environ.* **2021**, *750*, 141646. [CrossRef] [PubMed]
12. Wang, X.; Xie, H.; Guan, H.; Zhou, X. Different responses of MODIS-derived NDVI to root-zone soil moisture in semi-arid and humid regions. *J. Hydrol.* **2007**, *340*, 12–24. [CrossRef]
13. Bounoua, L.; Collatz, G.J.; Los, S.O.; Sellers, P.J.; Dazlich, D.A.; Tucker, C.J.; Randall, D.A. Sensitivity of Climate to Changes in NDVI. *J. Clim.* **2000**, *13*, 2277–2292. [CrossRef]
14. Buermann, W.; Dong, J.; Zeng, X.; Myneni, R.B.; Dickinson, R.E. Evaluation of the Utility of Satellite-Based Vegetation Leaf Area Index Data for Climate Simulations. *J. Clim.* **2001**, *14*, 3536–3550. [CrossRef]
15. Asbjornsen, H.; Goldsmith, G.R.; Alvarado-Barrientos, M.S.; Rebel, K.; Osch, F.P.V.; Rietkerk, M.; Chen, J.; Gotsch, S.; Tobón, C.; Geissert, D.R.; et al. Ecohydrological advances and applications in plant-water relations research: A review. *J. Plant Ecol.* **2011**, *4*, 3–22. [CrossRef]
16. Asbjornsen, H.; Ashton, M.S.; Vogt, D.J.; Palacios, S. Effects of habitat fragmentation on the buffering capacity of edge environments in a seasonally dry tropical oak forest ecosystem in Oaxaca, Mexico. *Agric. Ecosyst. Environ.* **2003**, *103*, 481–495. [CrossRef]
17. Potts, D.L.; Scott, R.L.; Bayram, S.; Carbonara, J. Woody plants modulate the temporal dynamics of soil moisture in a semi-arid mesquite savanna. *Ecohydrology* **2010**, *3*, 20–27. [CrossRef]
18. Wang, G.; Shen, Y.; Qian, J.; Wang, J. Study on the Influence of Vegetation Change on Soil Moisture Cycle in Alpine Meadow. *J. Glaciol. Geocryol.* **2003**, *25*, 653–659.
19. Zhang, Z.; Wu, G.; Wang, D.; Deng, L.; Hao, H.; Yang, Z.; Shangguan, Z. Plant com m unity structure and soilm oisture in the sem i -arid naturalgrassland of the Loess Plateau. *Acta Partaculturae Sin.* **2014**, *23*, 313–319.
20. Asbjornsen, H.; Shepherd, G.; Helmers, M.; Mora, G. Seasonal patterns in depth of water uptake under contrasting annual and perennial systems in the Corn Belt Region of the Midwestern, U.S. *Plant Soil* **2008**, *308*, 69–92. [CrossRef]
21. Lu, N.; Chen, S.; Wilske, B.; Sun, G. Evapotranspiration and soil water relationships in a range of disturbed and undisturbed ecosystems in the semi-arid Inner Mongolia, China. *J. Plant Ecol.* **2011**, *4*, 49–60. [CrossRef]
22. Schwinning, S. The ecohydrology of roots in rocks. *Ecohydrology* **2010**, *3*, 238–245. [CrossRef]
23. Zhang, Y.; Huang, D.; Zhao, X.; Zhao, S. Study on the potential evapotranspiration of grassland in the north slope of Qilianshan Mountain. *J. Anhui Agric. Sci.* **2008**, *36*, 8403–8405.
24. Volpe, V.; Marani, M.; Albertson, J.D.; Katul, G. Root controls on water redistribution and carbon uptake in the soil-plant system under current and future climate. *Adv. Water Resour.* **2013**, *60*, 110–120. [CrossRef]
25. Su, B.; Shangguan, Z. Decline in soil moisture due to vegetation restoration on the Loess Plateau of China. *Land Degrad. Dev.* **2019**, *30*, 290–299. [CrossRef]
26. Jia, X.; Shao, M.; Zhu, Y.; Luo, Y. Soil moisture decline due to afforestation across the Loess Plateau, China. *J. Hydrol.* **2017**, *546*, 113–122. [CrossRef]
27. Mao, J.; Nierop, K.G.J.; Damsté, J.S.S.; Dekker, S.C. Roots induce stronger soil water repellency than leaf waxes. *Geoderma* **2014**, *232–234*, 328–340. [CrossRef]
28. Santiago, L.S.; Goldstein, G.; Meinzer, F.C.; Fisher, J.B.; Machado, K.; Woodruff, D.; Jones, T. Leaf photosynthetic traits scale with hydraulic conductivity and wood density in Panamanian forest canopy trees. *Oecologia* **2004**, *140*, 543–550. [CrossRef]
29. Krauss, K.W.; Young, P.J.; Chambers, J.L.; Doyle, T.W.; Twilley, R.R. Sap flow characteristics of neotropical mangroves in flooded and drained soils. *Tree Physiol.* **2007**, *27*, 775–783. [CrossRef] [PubMed]
30. Bao, G.; Bao, Y.; Qin, Z.; Xin, X.; Bao, Y.; Bayarsaikan, S.; Zhou, Y.; Chuntai, B. Modeling net primary productivity of terrestrial ecosystems in the semi-arid climate of the Mongolian Plateau using LSWI-based CASA ecosystem model. *Int. J. Appl. Earth Obs. Geoinf.* **2016**, *46*, 84–93. [CrossRef]
31. Guo, L. Analyses the Soil Moisture of Mongolia Plateau with MODIS-TVDI MODEL and AMSR-E Data. Master's Thesis, Inner Mongolia Normal University, Hohhot, China, 2010.
32. Wei, B.; Shan, Y.; Jia, X.; Bao, Y.; Na, R.; Yin, S. Analysis of soil moisture retrieval and response to meteorological factors using AMSR-2. *Chin. J. Eco-Agric.* **2016**, *24*, 837–845.
33. Munkhtsetseg, E.; Shinoda, M.; Gillies, J.A.; Kimura, R.; King, J.; Nikolich, G. Relationships between soil moisture and dust emissions in a bare sandy soil of Mongolia. *Particuology* **2016**, *28*, 131–137. [CrossRef]
34. Maria, E.; Fernandez-Gimenez, B.; Allen, D. Testing a non-equilibrium model of rangeland vegetation dynamics in Mongolia. *J. Appl. Ecol.* **1999**, *36*, 871–885. [CrossRef]
35. Li, A.; Wu, J.; Huang, J.J.L.E. Distinguishing between human-induced and climate-driven vegetation changes: A critical application of RESTREND in inner Mongolia. *Landsc. Ecol.* **2012**, *27*, 969–982. [CrossRef]
36. Li, C.; Wang, J.; Hu, R.; Yin, S.; Bao, Y.; Ayal, D.Y. Relationship between vegetation change and extreme climate indices on the Inner Mongolia Plateau, China, from 1982 to 2013. *Ecol. Indic.* **2018**, *89*, 101–109. [CrossRef]
37. Wang, J.F.; Zhang, T.L.; Fu, B.J. A measure of spatial stratified heterogeneity. *Ecol. Indic.* **2016**, *67*, 250–256. [CrossRef]
38. Guo, E.; Wang, Y.; Wang, C.; Sun, Z.; Li, H. NDVI Indicates Long-Term Dynamics of Vegetation and Its Driving Forces from Climatic and Anthropogenic Factors in Mongolian Plateau. *Remote Sens.* **2021**, *13*, 688. [CrossRef]

39. Kang, J.; Bao, G.; Wu, L.; Zhang, W.; Jiang, L.; Liu, C. Variations in spring phenology of different vegetation types in the Mongolian Plateau and its responses to climate change during 2001–2017. *Chin. J. Ecol.* **2019**, *38*, 2490–2499.
40. Deng, Y.; Wang, S.; Bai, X.; Wu, L.; Cao, Y.; Li, H.; Wang, M.; Li, C.; Yang, Y.; Hu, Z.; et al. Comparison of soil moisture products from microwave remote sensing, land model, and reanalysis using global ground observations. *Hydrol. Process.* **2020**, *34*, 836–851. [CrossRef]
41. Kim, H.; Wigneron, J.P.; Kumar, S.; Dong, J.; Wagner, W.; Cosh, M.H.; Lakshmi, V. Global scale error assessments of soil moisture estimates from microwave-based active and passive satellites and land surface models over forest and mixed irrigated/dryland agriculture regions. *Remote Sens. Environ.* **2020**, *251*, 112052. [CrossRef]
42. Pinzon, J.E.; Tucker, C.J. A Non-Stationary 1981–2012 AVHRR NDVI3g Time Series. *Remote Sens.* **2014**, *6*, 6929–6960. [CrossRef]
43. Wang, J.; Dong, J.; Liu, J.; Huang, M.; Li, G.; Running, S.W.; Smith, W.K.; Harris, W.; Saigusa, N.; Kondo, H.; et al. Comparison of gross primary productivity derived from GIMMS NDVI3g, GIMMS, and MODIS in Southeast Asia. *Remote Sens.* **2014**, *6*, 2108–2133. [CrossRef]
44. Atkinson, P.M.; Jeganathan, C.; Dash, J.; Atzberger, C. Inter-comparison of four models for smoothing satellite sensor time-series data to estimate vegetation phenology. *Remote Sens. Environ.* **2012**, *123*, 400–417. [CrossRef]
45. Zhang, C.; Lei, T.; Song, D. Analysis of temporal and spatial characteristics of time lag correlation between the vegetation cover and soil moisture in the Loess Plateau. *Acta Ecol. Sin.* **2018**, *38*, 2128–2138.
46. Zhang, X.; Friedl, M.A.; Schaaf, C.B.; Strahler, A.H.; Hodges, J.C.F.; Gao, F.; Reed, B.C.; Huete, A. Monitoring vegetation phenology using MODIS. *Remote Sens. Environ.* **2003**, *84*, 471–475. [CrossRef]
47. Hou, X.; Gao, S.; Niu, Z.; Xu, Z. Extracting grassland vegetation phenology in North China based on cumulative spot-vegetation NDVI data. *Int. J. Remote Sens.* **2014**, *35*, 3316–3330. [CrossRef]
48. Wu, C.; Hou, X.; Peng, D.; Gonsamo, A.; Xu, S. Land surface phenology of China's temperate ecosystems over 1999–2013: Spatial-temporal patterns, interaction effects, covariation with climate and implications for productivity. *Agric. For. Meteorol.* **2016**, *216*, 177–187. [CrossRef]
49. Bao, G.; Chen, J.; Chopping, M.; Bao, Y.; Bayarsaikhan, S.; Dorjsuren, A.; Tuya, A.; Jirigala, B.; Qin, Z. Dynamics of net primary productivity on the Mongolian Plateau: Joint regulations of phenology and drought. *Int. J. Appl. Earth Obs. Geoinf.* **2019**, *81*, 85–97. [CrossRef]
50. Zhang, Z.; Shao, H.; Xu, P.; Chu, L.; Lu, Z.; Tian, J. On evolution and perspectives of bio-watersaving. *Colloids Surf. B Biointerfaces* **2007**, *55*, 1–9. [CrossRef]
51. Zhao, Z.; Shen, Y.; Wang, Q.; Jiang, R. The temporal stability of soil moisture spatial pattern and its influencing factors in rocky environments. *Catena* **2020**, *187*, 104418. [CrossRef]
52. Seneviratne, S.I.; Corti, T.; Davin, E.L.; Hirschi, M.; Jaeger, E.B.; Lehner, I.; Orlowsky, B.; Teuling, A.J. Investigating soil moisture–climate interactions in a changing climate: A review. *Earth Sci. Rev.* **2010**, *99*, 125–161. [CrossRef]
53. Teuling, A.J.; Troch, P.A. Improved understanding of soil moisture variability dynamics. *Geophys. Res. Lett.* **2005**, *32*, L05404. [CrossRef]
54. Guber, A.K.; Gish, T.J.; Pachepsky, Y.A.; Genuchten, M.T.V.; Daughtry, C.S.T.; Nicholson, T.J.; Cady, R.E. Temporal stability in soil water content patterns across agricultural fields. *Catena* **2007**, *73*, 125–133. [CrossRef]
55. Pachepsky, Y.A.; Guber, A.K.; Jacques, D. Temporal persistence in vertical distribution of soil moisture contents. *Soil Sci. Soc. Am. J.* **2005**, *69*, 347–352. [CrossRef]
56. Vanderlinden, K.; Pachepsky, Y.A.; Pederera-Parrilla, A.; Martínez, G.; Espejo-Pérez, A.J.; Perea, F.; Giráldez, J.V. Water Retention and Preferential States of Soil Moisture in a Cultivated Vertisol. *Soil Sci. Soc. Am. J.* **2017**, *81*, 1–9. [CrossRef]
57. Caldwell, M.M.; Richards, J.H. Hydraulic lift: Water efflux from upper roots improves effectiveness of water uptake by deep roots. *Oecologia* **1989**, *79*, 1–5. [CrossRef] [PubMed]
58. Dawson, T.E. Hydraulic lift and water use by plants: Implications for water balance, performance and plant-plant interactions. *Oecologia* **1993**, *95*, 565–574. [CrossRef] [PubMed]
59. Horton, J.L.; Hart, S.C. Hydraulic lift: A potentially important ecosystem process. *Trends Ecol. Evol.* **1998**, *8*, 232–235. [CrossRef]
60. Georg, J.; Helmut, S.; Herbert, H.; Gerhard, M.; Bernhard, K. A hillslope scale comparison of tree species influence on soil moisture dynamics and runoff processes during intense rainfall. *J. Hydrol.* **2012**, *420*, 112–124.
61. Koster, R.D.; Dirmeyer, P.A.; Guo, Z.; Bonan, G.; Chan, E.; Cox, P.; Gordon, C.T.; Kanae, S.; Kowalczyk, E.; Lawrence, D.; et al. Regions of Strong Coupling Between Soil Moisture and Precipitation. *Science* **2004**, *305*, 1138–1140. [CrossRef]
62. Li, H.; Wang, M.; Chai, B. Spatial and temporal characteristics of soil moisture dynamics in Loess Plateau. *J. Appl. Ecol.* **2003**, *14*, 14.
63. Zhang, Y.; Zhang, G. The analysis of soil moisture over typical mesa in the Chinese Loess Plateau. *J. Arid Land Resour. Environ.* **2010**, *24*, 190–195.
64. Liu, L.; Li, A.H.; Bao, Y.J.; Zhang, J.; Baoyin, T.; Zhou, Y.L. The corresponding relationship between the vertical root distribution of grassland communities and steppe degradation stage. *Chin. J. Grassl.* **2018**, *40*, 93–98.
65. Nathaly, R.G.; Mommer, L.; Grégoire, T.F.; Iversen, C.; Weigelt, A. Global root traits (groot) database. *Glob. Ecol. Biogeogr.* **2020**, *30*, 25–37.
66. Entin, J.K.; Robock, A.; Vinnikov, K.Y.; Hollinger, S.E.; Liu, S.; Namkhai, A. Temporal and spatial scales of observed soil moisture variations in the extratropics. *J. Geophys. Res. Atmos.* **2000**, *105*, 11865–11877. [CrossRef]

67. Pielke, R.A., Sr.; Avissar, R.; Raupach, M.; Dolman, A.J.; Zeng, X.; Denning, A.S. Interactions between the atmosphere and terrestrial ecosystems: Influence on weather and climate. *Glob. Chang. Biol.* **1998**, *4*, 461–475. [CrossRef]
68. Yang, W. Division of soil moisture status and afforestation problems in Loess Plateau. *Bull. Soil Water Conserv.* **1981**, *3*, 13–19.
69. Liu, S.; Yu, G.R.; Jun, A.; Michiaki, S.; Zhang, L.M.; Zhao, F.H.; Hu, Z.M.; Li, S.G. The thawing-freezing processes and soil moisture distribution of the steppe in central Mongolian Plateau. *Acta Pedol. Sin.* **2009**, *41*, 46–51.